agriculture

MDPI

Article

Enhancing Safety through Optimal Placement of Components in Hydrogen Tractor: Rollover Angle Analysis

Jinho Son [1], Yeongsu Kim [2], Seokho Kang [1] and Yushin Ha [1,2,*]

[1] Department of Bio-Industrial Machinery Engineering, College of Agriculture and Life Sciences, Kyungpook National University, Daegu 41566, Republic of Korea; thsghqkd@knu.ac.kr (J.S.); deshshk@knu.ac.kr (S.K.)
[2] Upland-Field Machinery Research Center, Kyungpook National University, Daegu 41566, Republic of Korea; mvio9256@naver.com
* Correspondence: yushin72@knu.ac.kr; Tel.: +82-53-950-5792

Abstract: Hydrogen tractors are being developed, necessitating consideration of the variation in the center of gravity depending on the arrangement of components such as power packs and cooling modules that replace traditional engines. This study analyzes the effects of component arrangement on stability and rollover angle in hydrogen tractors through simulations and proposes an optimal configuration. Stability is evaluated by analyzing rollover angles in various directions with rotations around the tractor's midpoint. Based on the analysis of rollover angles for Type 1, Type 2, and Type 3 hydrogen tractors, Type 2 demonstrates superior stability compared to the other types. Specifically, when comparing lateral rollover angles at 0° rotation, Type 2 exhibits a 2% increase over Type 3. Upon rotations at 90° and 180°, Type 2 consistently displays the highest rollover angles, with differences ranging from approximately 6% to 12% compared to the other types. These results indicate that Type 2, with its specific component arrangement, offers the most stable configuration among the three types of tractors. It is confirmed that the rollover angle changes based on component arrangement, with a lower center of gravity resulting in greater stability. These findings serve as a crucial foundation for enhancing stability in the future design and manufacturing phases of hydrogen tractors.

Keywords: hydrogen tractors; rollover; simulation

Citation: Son, J.; Kim, Y.; Kang, S.; Ha, Y. Enhancing Safety through Optimal Placement of Components in Hydrogen Tractor: Rollover Angle Analysis. *Agriculture* **2024**, *14*, 315. https://doi.org/10.3390/agriculture14020315

Academic Editor: Jin He

Received: 23 January 2024
Revised: 12 February 2024
Accepted: 13 February 2024
Published: 16 February 2024

1. Introduction

Owing to the increasing concerns associated with environmental issues and the depletion of fossil fuels, the shift from traditional fossil fuels to alternative energy sources such as solar power, hydrogen, and electricity is gaining momentum [1,2]. Likewise, in agriculture, awareness regarding environmental issues and sustainable energy is rapidly increasing. Also, conventional agricultural practices, which heavily depend on machinery using fossil fuels, have a considerable impact on greenhouse gas emissions and environmental pollution worldwide. These practices have resulted in substantial carbon emissions, water pollution, and soil degradation [3–5]. Consequently, performing research on the effective application of eco-friendly and sustainable energy sources to agriculture is imperative and can reduce dependence on conventional fossil fuels [6–8]. This could result in a paradigm shift from conventional internal combustion engines to alternative energy source tractors [9–11]. To further explore alternatives, Felseghi [12] conducted a comprehensive strengths, weaknesses, opportunities, and threats (SWOT) analysis to assess the feasibility of hydrogen as an alternative energy source. The analysis demonstrated that hydrogen fuel cell technology stands out as a promising solution for future clean energy systems. Additionally, tractors using hydrogen energy are more efficient for heavy-duty agricultural operations due to their high energy density and short charging times [13]. The development of hydrogen tractors, therefore, emerges as a strategically suitable direction to propel the agricultural sector towards a more eco-friendly paradigm.

When a new power source is developed and applied to tractors, it introduces unique considerations, including the reconfiguration of components and the optimization of energy storage systems. In the process of developing a new tractor that utilizes an alternative energy source, essential components for power transfer, such as the engine and transmission, need to be replaced. Instead, motors, batteries, supercapacitors, and fuel cell power systems must be employed [14,15]. Changes in the arrangement of key components during this transition may result in a shift in the center of gravity (CoG), potentially introducing new rollover risks. In the realm of developing tractors using alternative energy sources, it becomes crucial to conduct stability analyses based on the arrangement of each component. The dynamic characteristics of tractors using alternative energy sources vary based on component layout. Hence, performing stability analysis during the tractor development process is paramount [16–18].

One of the critical research areas for evaluating the stability of tractors is the rollover stability analysis, which is essential for protecting farmers from potential hazards during agricultural work and enhances tractor stability [19–21]. Moreover, considering the driving and operating environment of such vehicles, the demands for research on rollover in the agricultural tractor are soaring [22,23]. Thus, studies for proving the working boundary [24], evaluating stability behavior [25], and static or dynamic analysis using computational analysis methods have been performed so far [26,27]. Despite extensive research on tractor rollovers, tractor rollover accidents still account for a considerable proportion of agricultural machinery accidents [28,29]. Notably, tractor rollover accidents constitute the highest proportion of accidents within the agricultural sector, as reported by the U.S. Bureau of Labor Statistics [30]. Italy and Portugal, in particular, exhibit elevated rates of tractor rollover accidents and related fatalities [31,32]. Considering these statistics, additional research concentrating on the various factors associated with tractor rollover accidents becomes imperative. Rollover safety analysis stands out as a foundational research area in the endeavor to avert rollover accidents [33]. Research in this field primarily concentrates on both dynamic and static rollover analyses [34–36]. These studies play a role in proactive measures to prevent and alleviate tractor overturning accidents in agricultural environments, and accordingly, rollover stability analysis has been practically conducted.

Research is being actively conducted to evaluate stability through rollover stability analysis using simulation. Rollover stability analysis based on actual experiments is difficult considering the time, cost, and manpower required when experimenting in real life using a real tractor [37,38]. But, compared to an actual rollover experiment, rollover stability analysis through simulations is more advantageous as it is safer and easier to conduct research considering the time and cost. Variables can be set with a minimum time using simulations before proceeding with the actual experiment [39–41]. Chowdhury et al. [42] analyzed static rollover stability to reduce the risk of rollover in onion transplanters and deduced the lateral rollover angle in one direction. As the rollover angle was analyzed in only one direction, there was a limit to understanding the rollover angle in various directions. Kim et al. [43] derived various directions of rollover angle by analyzing simulations that used various rollover angles and situations to measure the rollover angle of the tractor more accurately in all directions. Furthermore, it was possible to analyze the dynamic as well as the static rollover angle [44] by installing various obstacles on the driving path in the simulation and to derive the rollover angle by setting various conditions attached to the tractor [45]. By conducting simulations under the application of various variables, experiments that are difficult in terms of time and cost can be efficiently conducted. Herein, the main components of a hydrogen tractor were considered, and a dynamic simulation was performed to analyze the rollover angle in different directions and arrangement of components.

This study aims to suggest the most stable placement of components that are alternatives to conventional fuel resources for the agricultural tractor. The CoG of the agricultural tractor was determined with different placement of components, then the rollover angle was analyzed using dynamic simulation software based on contact force. Rotating the

vehicle's vertical axle was considered due to covering a wide range of rollover incidents, and vehicle stability was evaluated with the load transfer ratio (LTR).

2. Material and Methods

2.1. 3D Model of a Tractor

The 3D model used in the rollover angle experiment of the hydrogen tractor was simplified by employing the specifications and basic form of a commercial 110-kW model. Recurdyn (2023, Function Bay Inc., Republic of Korea), a dynamic simulation, was used for the rollover simulation using a 3D model. The dimensions of the tractor used in the simulation were 4000 (L) × 2700 (W) × 2800 (H) mm, and the wheelbase was 2400 mm. The weight of the wheels was set to 110 kW. The front and rear wheel models were set to 385/85R28 and 460/85R38, their weights were set to 80 and 150 kg, respectively, and the total weight was set to 5100 kg (Table 1).

Table 1. Specifications of the hydrogen tractor.

Parameters	Values
Overall width (W)	2700 mm
Overall length (L)	4000 mm
Overall height (H)	2800 mm
Wheelbase	2400 mm
Mass of the front wheel	80 kg
Mass of the rear wheel	150 kg
Total mass of the tractor	5100 kg

2.2. Arrangement of the Main Components

In the development process of a hydrogen tractor, the engine mounted on the internal combustion tractor was set to E in the simulation to remove the engine mounted on the existing internal combustion tractor, replace it with the main component of the hydrogen tractor, and evaluate the stability of the tractor based on the component arrangement. P represents a 70-kW power pack, M represents a 95-kW motor, T represents a 51-L hydrogen tank, and CM represents a 70-kW cooling module. The width, length, and height of each component were shown in a simplified form and the weight was based on the weight of a product with similar specifications on the market (Table 2).

Table 2. Specifications of the main components in the tractor.

	E	P	M	T	CM
Width (mm)	870	1045	450	-	330
Height (mm)	1050	855	450	-	1430
Length (mm)	650	850	450	900	860
Diameter (mm)	-	-	-	350	-
Weight (kg)	550	250	80	36	250
Power (kW)	110	70	95	-	70

E = Engine; P = Power pack; M = Motor; T = Hydrogen tank; CM = Cooling module.

During the conversion of an existing internal combustion tractor into a hydrogen tractor, the engine of the internal combustion tractor should be removed and replaced with a power pack, motor, hydrogen tank, and cooling module, which are the main components of the hydrogen tractor. For this process, three arrangements of the main components in the internal combustion engine tractor and the hydrogen tractor equipped with the engine are shown in Figure 1.

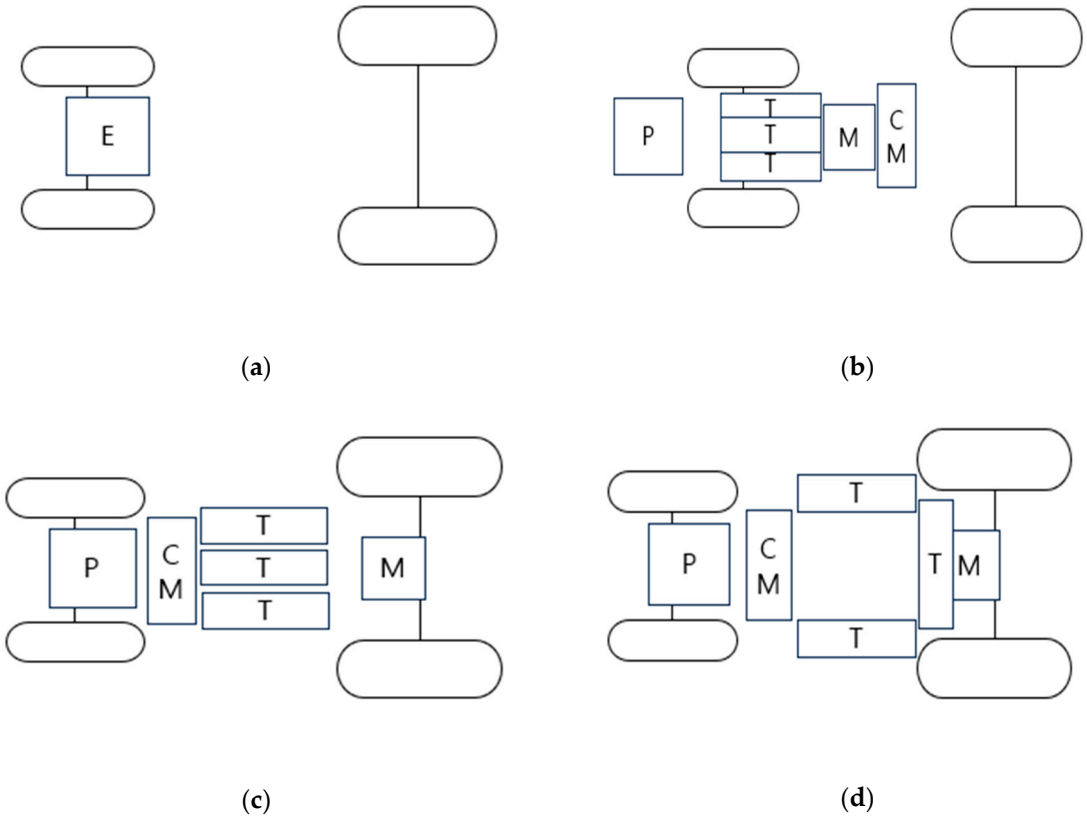

(**a**) (**b**)

(**c**) (**d**)

Figure 1. Layout of the main components in the combustion engine and hydrogen tractor: (**a**) Combustion engine tractor; (**b**) Type 1 hydrogen tractor; (**c**) Type 2 hydrogen tractor; and (**d**) Type 3 hydrogen tractor.

Within the simulation, the appearance of the internal combustion engine tractor equipped with the engine is shown in Figure 1a. The engine was removed and each Type was divided into three levels according to the arrangement of each main component in the hydrogen tractor. Figure 1b shows the Type 1 hydrogen tractor with a power pack, three hydrogen tanks, and a motor and a cooling module in the front. Figure 1c shows the Type 2 hydrogen tractor with a power pack instead of the existing engine, a cooling module, three hydrogen tanks in the front, and a motor in the rear. Figure 1d shows the Type 3 hydrogen tractor with a power pack and a cooling module instead of the existing engine, three hydrogen tanks on the tractor, and a motor in the rear.

Figure 2 shows the side view of each type of tractor, including the combustion tractor, and their orientation (0, 0 on XZ plane) where contact is made between the front wheel and the ground. The CoG of the combustion tractor was reflected in the 3D model based on a previous study that calculated the CoG with the overall dimensions of the vehicle [46]. This was then verified with the CoG calculation model that the software provided. After verifying the CoG of the combustion tractor, the engine was removed to permit placement of the components based on the three different types of tractors, and the CoG of each tractor was calculated with the CoG calculation model.

Table 3 summarizes the center of gravity (CoG) coordinates of each tractor and the front-to-rear CoG ratio. The CoG coordinates of a conventional internal combustion engine tractor were (1355.7, 1356.59), and the front-to-rear CoG ratio of the tractor was 0.56:0.44. Subsequently, the CoG of the internal combustion engine tractor was recalculated to remove the engine and replace it with a component mounted on the hydrogen tractor. After the engine was removed, the CoG coordinates of the tractor were (1461.48, 1375.94), and the front-to-rear CoG ratio was 0.61:0.39. The CoG coordinates of Type 1 were (1245.66, 1345.39), and its front-to-rear CoG ratio was 0.52:0.48. The CoG coordinates of Type 2 were (1373.53, 1348.7), and the front-to-rear CoG ratio was 0.57:0.43. The CoG coordinates of Type 3 were

(1381.42, 1388.64), and the front-to-rear CoG ratio was 0.58:0.42. Type 1 exhibited the lowest CoG height of 1345.39, while Type 3 exhibited the highest CoG height of 1388.64.

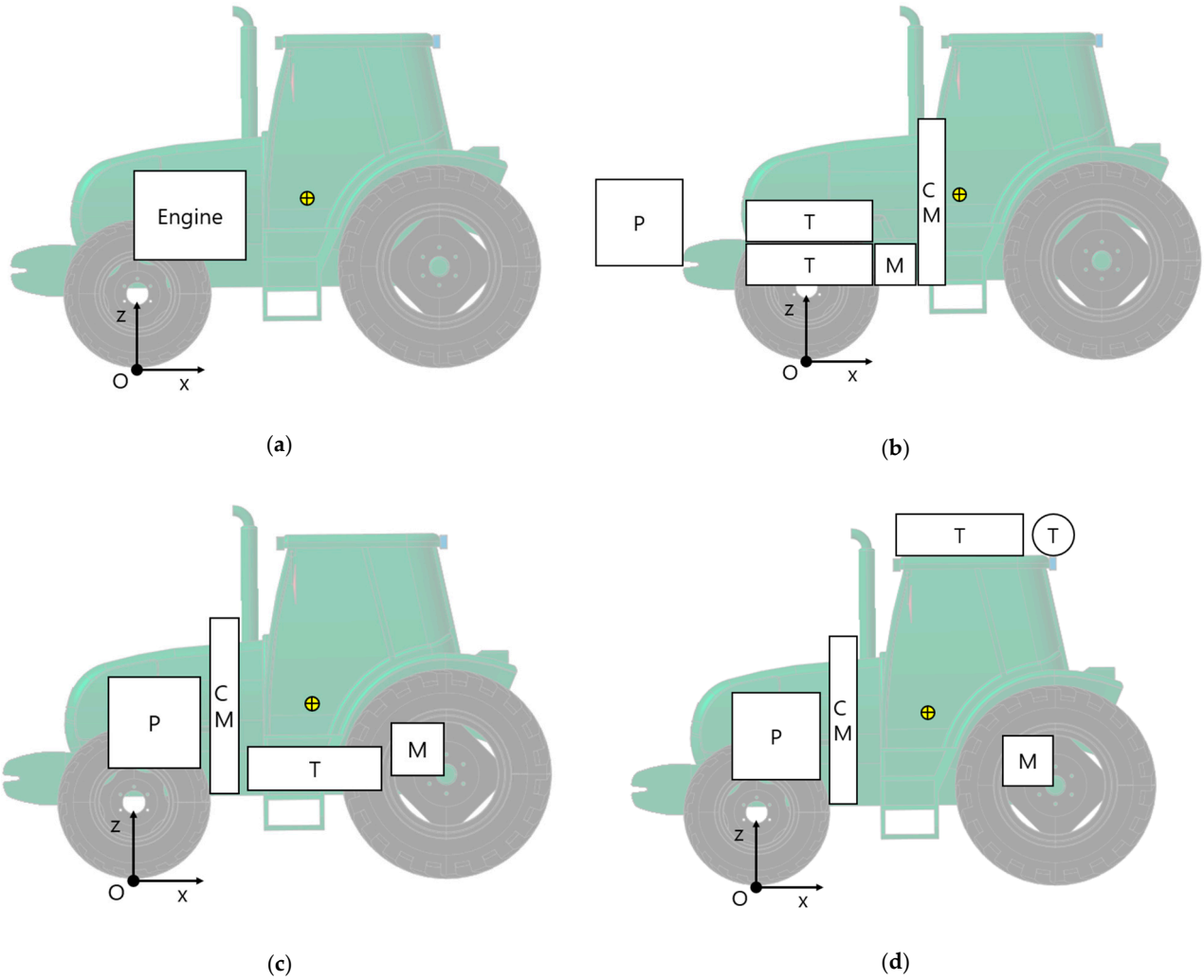

Figure 2. Displacement of the main components of the combustion engine and hydrogen tractor in the simulation: (**a**) Combustion engine tractor; (**b**) Type 1 hydrogen tractor; (**c**) Type 2 hydrogen tractor; (**d**) Type 3 hydrogen tractor.

Table 3. Each tractor's center of gravity coordinates and ratio.

	Combustion Tractor	Type 1	Type 2	Type 3
X coordinate	1355.72	1245.66	1373.53	1381.42
Z coordinate	1356.59	1345.39	1348.7	1388.64
Center of gravity ratio	0.56:0.44	0.52:0.48	0.57:0.43	0.58:0.42

2.3. Mathematical Model of the Tractor Rollover

The rollover motion used in this study can be expressed with the mathematical model shown in Figure 3. G represents the CoG of the tractor, h is the vertical distance from the ground to the CoG, θ_r is the lateral angle, a is the distance between the CoG and the y-axis, b is the distance between the front wheel and the CoG, c is the distance between the rear wheel and the CoG. A and B represent the intersection point of the ground and left wheels (rear and front, respectively), and E and F are the right wheels (rear and front, respectively). C, D, and K represent the intersection point of the center plane of the vehicle and the bottom

plane created with A, B, E, and F (front, middle, and rear, respectively). L represents the wheelbase, M is the intersection point of the front frame and center plane of the vehicle, H is the height of M. J represents the intersection point of line AM and the projected vertical line of G to line AM. I represents the intersection point of line MD and the projected vertical line of G to line MD (Figure 3). The tractor overturns when the position of the CoG crosses the wheelbase as the position of the CoG moves or the angle of inclination is greater than the critical angle [44]. Considerations for dynamic analysis include defining CoG through equations, as the CoG changes depending on the selected component arrangement. In this study, the front axle and the tractor frame were viewed as one. Therefore, the front axle cannot move separately. The tractor used does not have suspension for ease of calculating the change in CoG. This assumption may affect the tractor balance but was not considered in this rollover angle test [43].

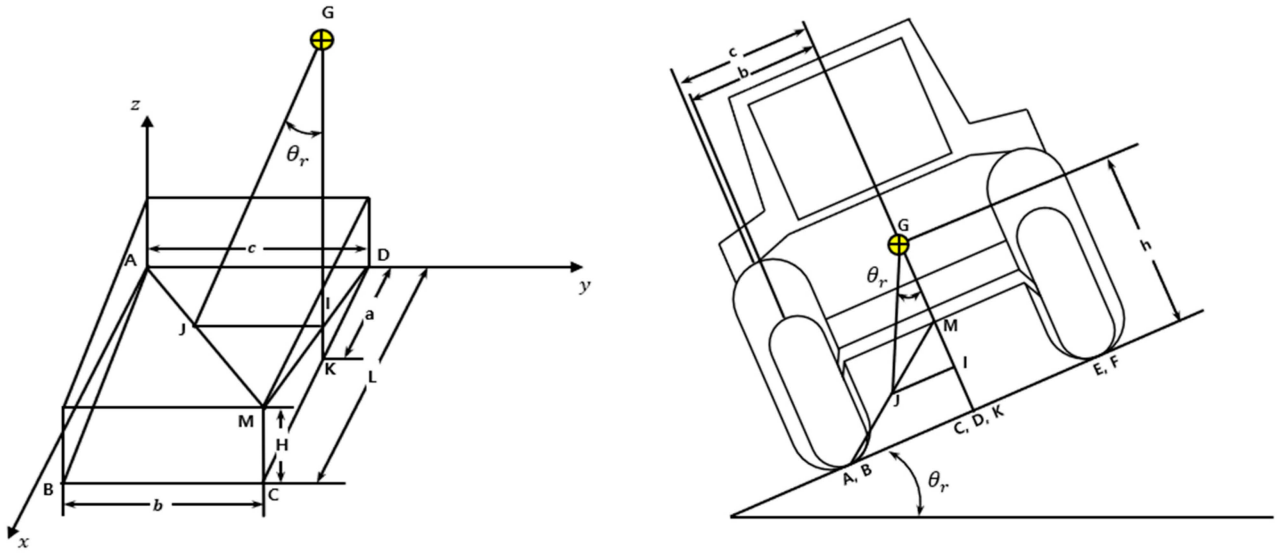

(**a**) (**b**)

Figure 3. Schematic diagram of rollover of tractor: (**a**) Normal condition; (**b**) Tilting condition.

It is assumed that the center of gravity G (a, c, h) of the tractor is located on the line of AM. To calculate G when the tractor is tilted and overturns, $G'\left(X_{cog}{}', Y_{cog}{}', Z_{cog}{}'\right)$ is newly assumed on the AB line (Figure 4). α and β are determined to be Equations (1) and (2).

$$\alpha = \tan^{-1}\frac{c}{L} \tag{1}$$

$$\beta = \tan^{-1}\frac{H}{\sqrt{L^2 + c^2}} \tag{2}$$

Here, α is an angle of change from the y-axis to the Y-axis, and β is an angle of change from the z-axis to the Z-axis.

To determine the new G′, the transformation from the xyz coordinate system to the XYZ coordinate system is determined by Equation (3).

$$\begin{bmatrix} X \\ Y \\ Z \end{bmatrix} = \begin{bmatrix} \cos\alpha\cos\beta & -\sin\alpha\cos\beta & -\sin\beta \\ -\sin\alpha & \cos\alpha & 0 \\ -\cos\alpha\sin\beta & \sin\alpha\sin\beta & \cos\beta \end{bmatrix} \begin{bmatrix} x \\ y \\ z \end{bmatrix} \tag{3}$$

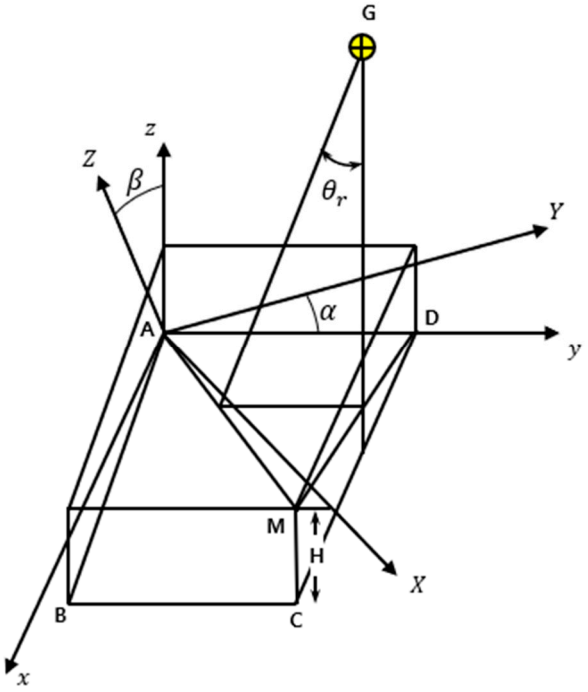

Figure 4. Diagram showing new coordinate system for different angles from xyz to XYZ.

The conversion of CoG in the XYZ coordinate system is determined by Equation (4) from xyz (G (*a*, *c*, *h*)) to XYZ ($G(X_{cog}, Y_{cog}, Z_{cog})$).

$$\begin{bmatrix} Xcog \\ Ycog \\ Zcog \end{bmatrix} = \begin{bmatrix} \cos\alpha\cos\beta & -\sin\alpha\cos\beta & -\sin\beta \\ -\sin\alpha & \cos\alpha & 0 \\ -\cos\alpha\sin\beta & \sin\alpha\sin\beta & \cos\beta \end{bmatrix} \begin{bmatrix} a \\ c \\ h \end{bmatrix} \quad (4)$$

After that, the initial $G(X_{cog}, Y_{cog}, Z_{cog})$ obtained from the XYZ coordinate system can be calculated through Equations (5)–(7) by using the tractor rotation angle ω to calculate the changing $G'(X_{cog}', Y_{cog}', Z_{cog}')$.

$$X_{cog}' = X_{cog} \quad (5)$$

$$Y_{cog}' = Y_{cog}\cos\omega - Z_{cog}\sin\omega \quad (6)$$

$$Z_{cog}' = Y_{cog}\sin\omega - Z_{cog}\sin\omega \quad (7)$$

2.4. Simulation Conditions and Method

Computational analysis was performed with the software Recurdyn (V2023) in this study. For repeated simulation, several constant parameters should be determined based on the previous study [47] and they were summarized in Table 4. The dynamic friction coefficient between the road surface and tire was 1.2. The stiffness and damping coefficients were 105 and 10, respectively. The simulation time and step were determined to be 25 s and 1000, respectively, and the rollover speed was 0.04 rad/s in this study. The results are compared to each other while the general agricultural machinery inspection standard value was also considered for the evaluation [48].

Table 4. Variable parameters for the simulation.

Parameters	Values
Dynamic friction coefficient	1.2
Stiffness coefficient	105
Damping coefficient	10
Simulation time	25 s
Simulation steps	1000

Figure 5 represents the schematic diagram of the rollover simulation. The simulation methodology and considered assumption are expressed in Figure 6. The simulation was performed as follows:

1. The tractor was placed on the ground plane,
2. The ground plane started to rotate with a pivot point at the corner,
3. Tilted the ground at 0.04 rad/s,
4. The rollover angle was analyzed when the contact force between the left two wheels and the ground became 0 N,
5. Then, it was repeated by turning the tractor 15° counterclockwise based on the midpoint (Figure 5b).

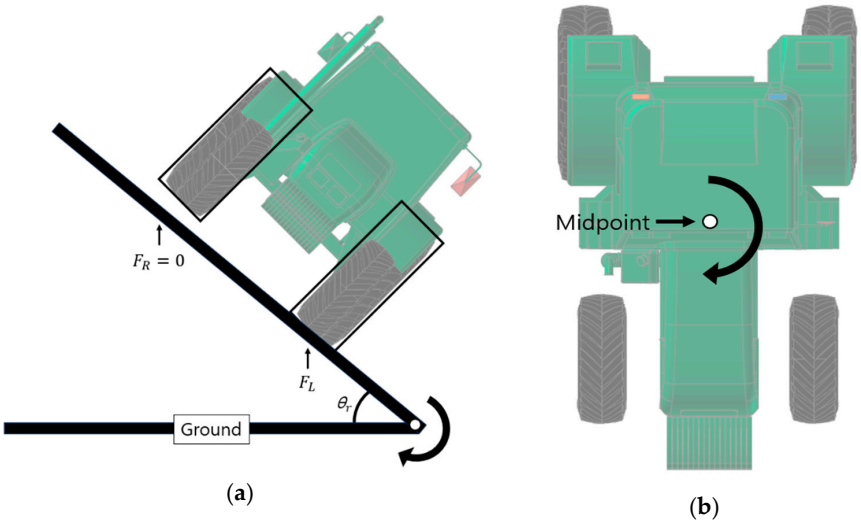

(**a**) (**b**)

Figure 5. Schematic view of simulation method: (**a**) Critical condition (**b**) Rotate method.

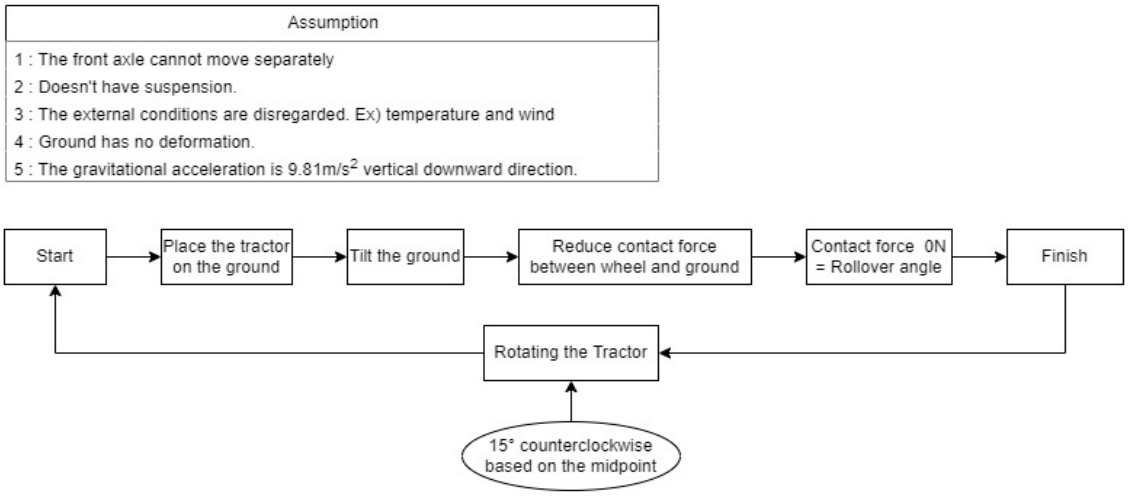

Figure 6. Flow chart of simulation methodology and assumptions considered in this study.

2.5. Load Transfer Ratio (LTR) Indicator for Tractor Rollover

The Load Transfer Ratio (LTR) evaluation method is widely used to evaluate vehicle rollover stability [49,50]. This paper also intends to additionally evaluate the presentation of the existing rollover angle through the rollover evaluation method based on LTR.

The LTR was defined as the ratio of the difference between the vertical loads of the left and right wheels and the total vertical loads.

$$LTR = \left| \frac{F_L - F_R}{F_L + F_R} \right| \tag{8}$$

where F_L is the load of the left wheels, F_R is the load of the right wheels.

In addition, it was intended to evaluate the overturning of the tractor using the load transfer ratio back and forth by expanding it into a situation where the left and right sides were overturned.

$$LTR = \left| \frac{F_f - F_r}{F_f + F_r} \right| \tag{9}$$

where F_f is the load of the front wheels, F_r is the load of the rear wheels.

The value of the LTR appears from 0 to 1 and means that the probability of overturning is higher as it goes to 1.

3. Results

3.1. Comparison Rollover Angle of the Tractor after Simulation

Figure 7 shows the result of the lateral rollover simulation of the internal combustion engine tractor at a rotation angle of 0°. The graph in the figure shows the contact force between each wheel and the ground. The X and Y axes represent the tilt angle of the ground and the contact force between the ground and each wheel, respectively. The contact force between the left front and rear wheels gradually increased, and the right front and rear wheels gradually decreased; therefore, the Rollover angle became 35.89° at 0 N.

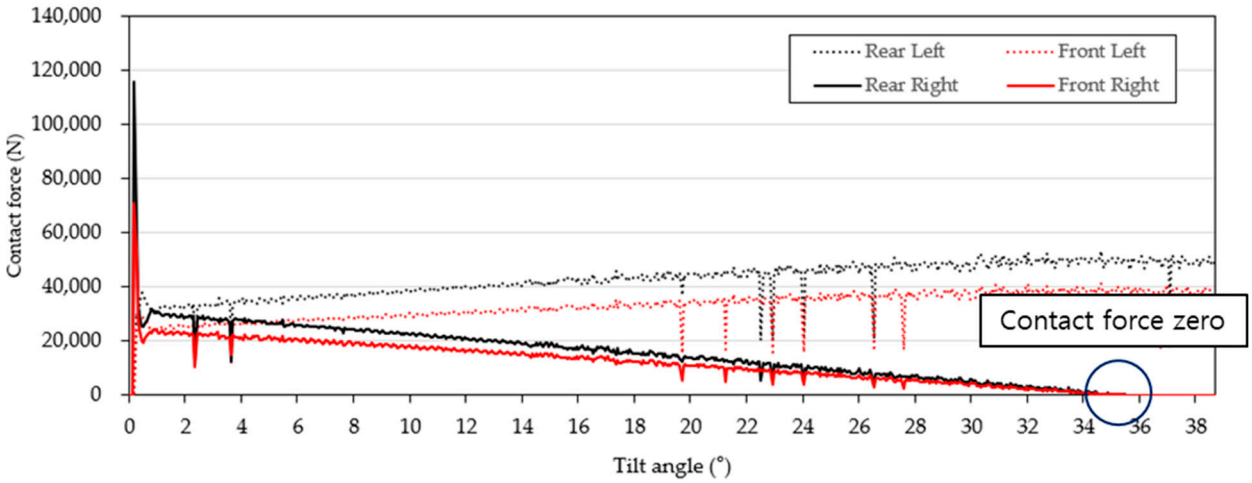

Figure 7. Contact force as a function of the rollover angle of the tractor.

Figure 8 depicts the graph illustrating the rollover angles of the conventional internal combustion engine tractor upon rotation by 15° increments. Upon rotation at 0°, 90°, 180°, and 270°, the rollover angles for the left side, front, right side, and rear were found to be 35.89°, 45.51°, 36.51°, and 38.25°, respectively. This value satisfies the agricultural machinery safety standard of 30° [48]. The highest rollover angle was 49.9° when the tractor was rotated by 120°, whereas the lowest rollover angle was 35.89° when the tractor was rotated by 0°.

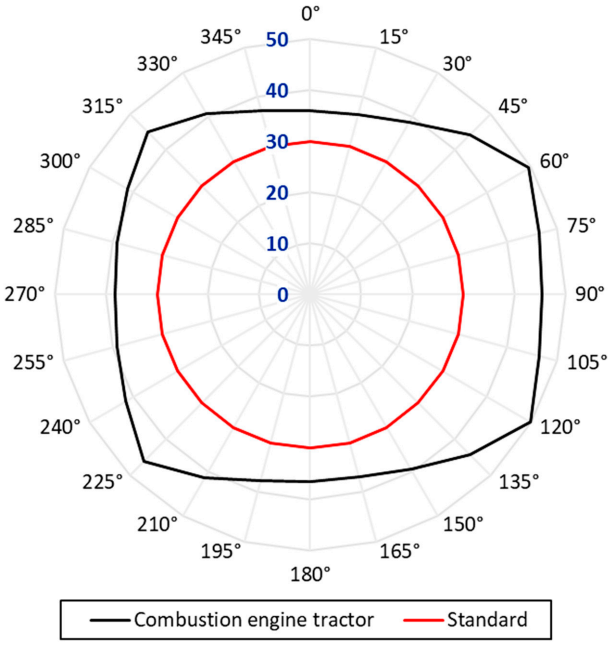

Figure 8. Comparison of the rollover angles of the combustion engine tractor and the standard (Blue letter: rollover angle, Black letter: rotation angle).

Figure 9 plots the rollover angles of the Type 1, Type 2, and Type 3 hydrogen tractors in all directions. First, the lateral rollover angles of the three tractors were compared upon rotation at 0°: Type 1, Type 2, and Type 3 tractors exhibited lateral rollover angles of 36.0°, 36.14°, and 35.33°, respectively. The rollover angle of Type 2 was 2% greater than that of Type 3. Next, when each type was rotated by 90°, 180°, and 270°, the rollover angles of the front, right side, and rear were determined. Upon rotations of 90°, 180°, and 270°, Type 1 exhibited rollover angles of 43.31°, 36.51°, and 41.23°, respectively. For Type 2, these rollover angles were 46.01°, 36.62°, and 37.97°, respectively. The corresponding values for Type 3 were 45.34°, 35.83°, and 36.96°.

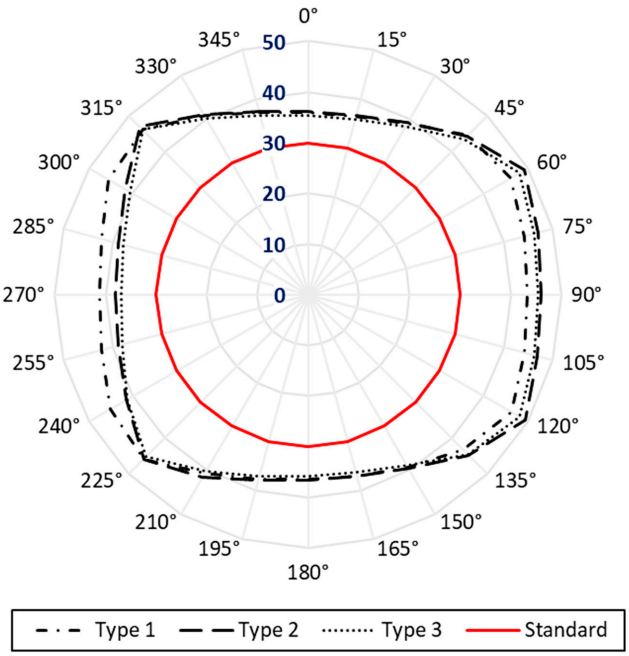

Figure 9. Comparison of the rollover angles of each type of tractor and the standard (Blue letter: rollover angle, Black letter: rotation angle).

Table 5 shows the rollover angle for each type in a tabular form. Yellow represents the highest rollover angle for each rotation angle, and blue represents the lowest rollover angle for each rotation angle. Relative change is the difference between the highest rollover angle and the lowest rollover angle.

Table 5. Tabular chart of rollover angles for combustion engine tractor and each type.

Rotate Angle (°)	Combustion Engine Tractor (°)	Type 1 (°)	Type 2 (°)	Type 3 (°)	Relative Change
0	35.89	36.00	36.14	35.33	2%
15	36.34	36.45	36.56	35.83	2%
30	38.87	38.93	39.15	38.25	2%
45	44.27	44.55	44.33	43.43	3%
60	49.50	46.18	49.28	48.09	7%
75	46.46	44.27	46.97	46.24	6%
90	45.51	43.31	46.01	45.34	6%
105	46.52	44.16	46.91	46.24	6%
120	49.9	46.41	49.50	48.26	7%
135	44.21	43.15	44.78	44.72	4%
150	39.49	39.43	39.60	38.81	2%
165	36.96	37.01	37.13	36.34	2%
180	36.51	36.51	36.62	35.83	2%
195	37.74	37.80	37.91	37.13	2%
210	41.35	40.67	41.68	40.33	3%
225	46.07	45.90	45.96	45.23	2%
240	41.68	45.17	41.40	41.35	9%
255	39.15	42.19	38.87	37.97	11%
270	38.25	41.23	37.97	36.96	12%
285	39.15	42.19	38.81	37.80	12%
300	41.35	45.51	41.80	40.67	12%
315	44.94	46.24	46.86	46.07	2%
330	40.78	40.73	41.06	40.22	2%
345	37.18	37.29	37.46	36.62	2%

Notably, upon rotation at 90°, Type 2 exhibited the highest rollover angle of 46.01°, while Type 1 exhibited the lowest rollover angle of 43.31°, a difference of approximately 6%. Upon rotation at 180°, Type 2 again exhibited the highest rollover angle of 36.62°, whereas Type 3 exhibited the lowest rollover angle of 35.83°, a difference of approximately 2%. Upon rotation at 270°, Type 1 exhibited the highest rollover angle of 41.23°, while Type 3 exhibited the lowest value rollover angle of 36.96°, indicating a difference of approximately 12%.

Although small differences in rollover angles were observed in the lateral direction for all types of tractors, significant differences of approximately 6% and 12% were observed in the front and rear rollover angles, respectively. Specifically, Type 2 exhibited the highest stability in the frontal rollover, while Type 1 exhibited the highest stability in the rear rollover.

By averaging the rollover angles across all rotation directions for each type, Type 1, Type 2, and Type 3 exhibited average rollover angles of 41.7°, 41.8°, and 41.0°.

Consequently, Type 2 exhibited the highest average rollover angle, while Type 3 exhibited the lowest rollover angle, with a difference of approximately 2%. Comparing the types based on the average rollover angle, Type 2 clearly exhibited the most stable arrangement of the components.

Finally, the comprehensive comparison of the three types of tractors in each rotation direction revealed that Type 3 exhibited the most instances of low rollover angles, whereas Type 2 exhibited the most instances of high rollover angles. Compared to Types 1 and 2, Type 3, with a CoG height of 1388.64, exhibited lower rollover angles, indicating its instability. Types 1 and 2 exhibited similar CoG heights, but for Type 2, its CoG was positioned further back. Consequently, during inclination where the CoG moved upward (60° to 135°), Type 2 exhibited higher rollover angles, while during inclination where the CoG shifted downward (240° to 300°), Type 1 exhibited higher rollover angles. Considering the stability of the hydrogen tractor by its potential for rollover, placing the components according to the same arrangement as shown in Type 2 was found to be the most stable.

The CoG heights for Type 1 and Type 2 were similar, but the distribution of weight toward the front and rear differed. When the CoG of the tractor was situated below a slope, having the CoG toward the rear posed higher risks.

3.2. Load Transfer Ratio (LTR) Analysis for Each Type of Tractor

Furthermore, Figure 10 shows the LTR comparison graphs to present various perspectives on the rollover angle obtained in Figure 9. The *X*-axis is the time of simulation, *Y*-axis is LTR. At 0° and 180°, the rollover angles are similar for all types. However, at 90° and 270°, significant differences are evident. At 90°, Type 1 achieves overturning most rapidly, while Types 2 and 3 overturned at similar points in time. At 270°, Types 2 and 3 overturned at similar times, with Type 1 experiencing the latest overturning. These results emphasize the importance of balancing the weight distribution between the front and rear when arranging components. When designing a tractor, the CoG should be properly positioned to show the vulnerability of overturning when positioned downward from the CoG when the CoG is overturned to the front and rear.

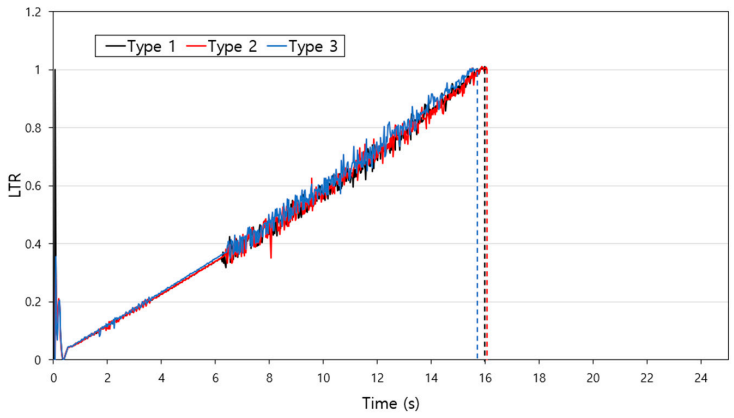

(**a**)

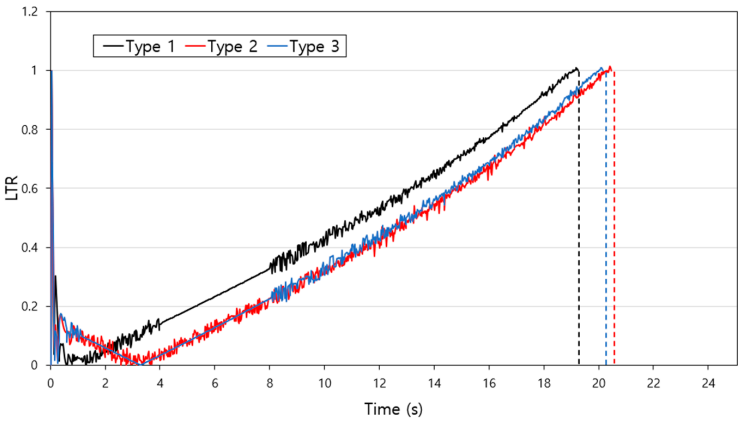

(**b**)

Figure 10. *Cont.*

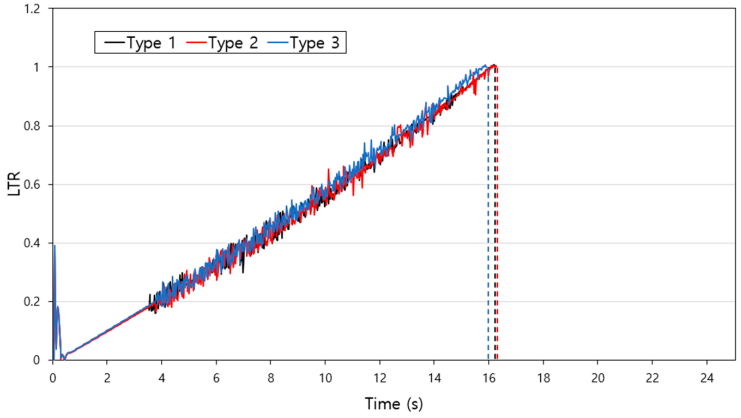

(**c**)

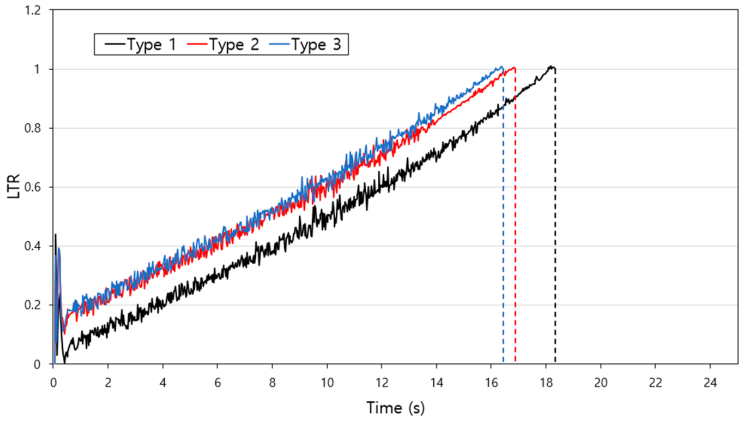

(**d**)

Figure 10. The LTR analysis for rotation angle of hydrogen tractor: (**a**) 0°, (**b**) 90°, (**c**) 180°, (**d**) 270°.

Placing the hydrogen tank on the top of the tractor, as shown in Type 3, increased the CoG, thereby reducing the stability of the tractor. The proportion of weight distribution between the front and rear affected the handling of the tractor during rotation and when entering sloped areas, while the CoG height impacted tractor handling in all directions.

4. Discussion

We investigated the effects of main component arrangement on the stability of hydrogen tractors using simulations. Our experimental findings revealed that Type 2 tractors exhibited higher average rollover angles and rollover angles in various directions compared to other types. Moreover, our study highlighted the importance of a lower CoG and appropriate weight distribution between the front and rear for tractor stability.

Comparing our results with the related literature, agricultural machinery is more prone to overturning when the CoG is positioned higher [51]. Lee et al. [52] found that the stability against overturning increases as the center of gravity moves forward and the full width of the vehicle increases, but this study analyzed one direction. In this study, conducting an experiment on the overturning angle from various directions, it is judged that the position of the CoG is important but the overturning angle according to the appropriate position of the front and rear ratio of the CoG should also be considered. According to the agricultural machine test standards, the overturning angle should be at least 30° [48]. However, Kim et al. [43] found that the minimum longitudinal overturning was 29.19°~33.25°. Furthermore, according to ISO 16251-2 [53], the allowable range of the overturning angle depending on the off-road agricultural machine is 15°~45°. All three proposed types of hydrogen tractors met the criteria for the overturning angle.

However, high stability is not the only advantage required for agriculture. Considering the agricultural tractor was designed to perform work requiring high power, moving the CoG backward might result in reduced operating capability. Therefore, the CoG should be placed forward and close to the ground in order to maintain operating capability and stability at the same time. Furthermore, we did not fully consider real-world issues such as interference from arbitrary component placements and performance reduction due to component heating. Additionally, relying solely on simulations for rollover angle testing may introduce errors compared to real tractor rollover experiments. Therefore, future research should include experiments with actual hydrogen tractors to better understand stability and rollover angles based on main component placement.

Furthermore, there is a need to optimize CoG distribution and component placement to enhance tractor stability while ensuring efficient operation. Addressing these aspects through further research can significantly contribute to the design and stability enhancement of hydrogen tractors, thereby improving their efficiency and safety. Additionally, policy discussions may arise regarding regulations or standards for hydrogen tractor designs and testing, further emphasizing the importance of our findings.

5. Conclusions

In this study, the effect of replacing the conventional components of agricultural tractors with different placements was analyzed using Recurdyn. The CoG of combustion engine tractors was analyzed and verified first, then three types of tractors were created with different arrangements of components and the CoG of each tractor was analyzed. Subsequently, the rollover angle defined as zero newton of contact force between the wheels and the ground plane was analyzed and the simulation was repeated by turning the tractor 15° on its vertical axis. Finally, a comparison of the stability between each type was performed.

The component placement of Type 2 had the highest stability among all types of tractors. It had a maximum rollover angle of 49.5° at a rotation angle of 120°. Also, it showed the highest rollover angle at most of the rotation angles among all types of tractors, with an average rollover angle of 41.8° for every rotation angle. Generally, the lower the CoG is located, the higher stability is shown. However, when the rotation angle is taken into account, the location of CoG on the longitude axis should be considered. As a result, the lowest height of CoG was observed in Type 2 and located in a forward position compared with the other types of tractors. Therefore, the arrangement of components observed in Type 2 can be suggested for the agricultural tractor using alternative components.

Furthermore, additional research is required to optimize the distribution of the CoG and the placement of the components to enhance tractor stability while ensuring efficient operation. Such research can significantly contribute to the design and stability improvement of hydrogen tractors, ultimately enhancing their efficiency and safety. Also, consideration of parameters such as tire elasticity, damping coefficient, and analyzing dynamic motion should be performed in future research.

Author Contributions: Conceptualization, J.S. and Y.K.; methodology, S.K.; software, J.S.; validation, J.S.; analysis, J.S.; writing—original draft preparation, J.S. and S.K.; writing—review and editing, J.S. and S.K.; visualization, J.S.; supervision, Y.H.; project administration, Y.H.; funding acquisition, Y.H. All authors have read and agreed to the published version of the manuscript.

Funding: This work was supported by the Korea Institute of Planning and Evaluation for Technology in Food, Agriculture and Forestry (IPET) through Eco-friendly Power Source Application Agricultural Machinery Technology Development Program, funded by Ministry of Agriculture, Food and Rural Affairs (MAFRA) (322047-5).

Institutional Review Board Statement: Not applicable.

Informed Consent Statement: Not applicable.

Data Availability Statement: Data is contained within the article.

Conflicts of Interest: The authors declare no conflicts of interest.

References

1. Faria, R.; Moura, P.; Delgado, J.; De Almeida, A.T. A sustainability assessment of electric vehicles as a personal mobility system. *Energy Convers. Manag.* **2012**, *61*, 19–30. [CrossRef]
2. Owusu, P.A.; Asumadu, S.S. A review of renewable energy sources, sustainability issues and climate change mitigation. *Cogent Eng.* **2016**, *3*, 1167990. [CrossRef]
3. Gonzalez-de-Soto, M.; Emmi, L.; Benavides, C.; Garcia, I.; Gonzalez-de-Santos, P. Reducing air pollution with hybrid-powered robotic tractors for precision agriculture. *Biosyst. Eng.* **2016**, *143*, 79–94. [CrossRef]
4. Moreda, G.P.; Muñoz-García, M.A.; Barreiro, P.J.E.C. High voltage electrification of tractor and agricultural machinery—A review. *Energy Convers. Manag.* **2016**, *115*, 117–131. [CrossRef]
5. Mocera, F.; Somà, A. Analysis of a parallel hybrid electric tractor for agricultural applications. *Energies* **2020**, *13*, 3055. [CrossRef]
6. Malik, A.; Kohli, S. Electric tractors: Survey of challenges and opportunities in India. *Mater. Today Proc.* **2020**, *28*, 2318–2324. [CrossRef]
7. Van Leeuwen, L.B. *Hydrogen or Battery Tractors: What Potential for Sustainable Grape Growing?* IVES Technical Reviews; Vine and Wine: Villenave d'Ornon, France, 2020.
8. Ghobadpour, A.; Monsalve, G.; Cardenas, A.; Mousazadeh, H. Off-road electric vehicles and autonomous robots in agricultural sector: Trends, challenges, and opportunities. *Vehicles* **2022**, *4*, 843–864. [CrossRef]
9. Ettl, J.; Thuneke, K.; Remmele, E.; Emberger, P.; Widmann, B. Future biofuels and driving concepts for agricultural tractors. In Proceedings of the 2014 European Biomass Conference and Exhibition, Hamburg, Germany, 24–27 June 2014; pp. 23–25.
10. Sassetti, R.; Ferrante, S.; Lenzini, N.; Nuzzo, S.; Fiorati, S.; Barater, D. Potential of Powertrain Electrification in a mid-size Tractor for a more sustainable agriculture. In Proceedings of the 2023 AEIT International Conference on Electrical and Electronic Technologies for Automotive, Modena, Italy, 17–19 July 2023; pp. 1–6.
11. Jia, C.; Qiao, W.; Qu, L. Modeling and control of hybrid electric vehicles: A case study for agricultural tractors. In Proceedings of the 2018 IEEE Vehicle Power and Propulsion Conference, Chicago, IL, USA, 27–30 August 2018; pp. 1–6.
12. Felseghi, R.A.; Carcadea, E.; Raboaca, M.S.; Trufin, C.N.; Filote, C. Hydrogen fuel cell technology for the sustainable future of stationary applications. *Energies* **2019**, *12*, 4593. [CrossRef]
13. Handwerker, M.; Wellnitz, J.; Marzbani, H. Comparison of hydrogen powertrains with the battery powered electric vehicle and investigation of small-scale local hydrogen production using renewable energy. *Hydrogen* **2021**, *2*, 76–100. [CrossRef]
14. Xu, L.; Liu, M.; Zhou, Z. Design of drive system for series hybrid electric tractor. *Trans. Chin. Soc. Agric. Eng.* **2014**, *30*, 11–18.
15. Baek, S.Y.; Kim, W.S.; Kim, Y.S.; Kim, Y.J.; Park, C.G.; An, S.C.; Kim, B.S. Development of a simulation model for an 80 kW-class electric all-wheel-drive (AWD) tractor using agricultural workload. *J. Drive Control* **2020**, *17*, 27–36.
16. Ueka, Y.; Yamashita, J.; Sato, K.; Doi, Y. Study on the development of the electric tractor: Specifications and traveling and tilling performance of a prototype electric tractor. *Eng. Agric. Environ. Food* **2013**, *6*, 160–164. [CrossRef]
17. Gao, H.; Xue, J. Modeling and economic assessment of electric transformation of agricultural tractors fueled with diesel. *Sustain. Energy Technol. Assess.* **2020**, *39*, 100697. [CrossRef]
18. Mello, R.R.; Antunes, F.L.; Daher, S.; Vogt, H.H.; Albiero, D.; Tofoli, F.L. Conception of an electric propulsion system for a 9 kW electric tractor suitable for family farming. *IET Electr. Power Appl.* **2019**, *13*, 1993–2004. [CrossRef]
19. Sanderson, W.T.; Madsen, M.D.; Rautiainen, R.; Kelly, K.M.; Zwerling, C.; Taylor, C.D.; Merchant, J.A. Tractor overturn concerns in Iowa: Perspectives from the Keokuk county rural health study. *J. Agric. Saf. Health* **2006**, *12*, 71–81. [CrossRef] [PubMed]
20. Myers, M.L.; Cole, H.P.; Westneat, S.C. Injury severity related to overturn characteristics of tractors. *J. Saf. Res.* **2009**, *40*, 165–170. [CrossRef] [PubMed]
21. Murphy, D.J.; Myers, J.; McKenzie, E.A., Jr.; Cavaletto, R.; May, J.; Sorensen, J. Tractors and Rollover Protection in the United States. *J. Agromed.* **2010**, *15*, 249–263. [CrossRef] [PubMed]
22. He, Z.; Song, Z.; Wang, L.; Zhou, X.; Gao, J.; Wang, K.; Yang, M.; Li, Z. Fasting the stabilization response for prevention of tractor rollover using active steering: Controller parameter optimization and real-vehicle dynamic tests. *Comput. Electron. Agric.* **2023**, *204*, 107525. [CrossRef]
23. Carabin, G.; Becce, L.; Mazzetto, F. Development and Experimental Evaluation of a Tractor Roll-Over Stability Model. In Proceedings of the 2022 Conference of the Italian Society of Agricultural Engineering, Palermo, Italy, 19–22 September 2022; Springer International Publishing: Cham, Switzerland, 2022; pp. 429–436.
24. Kang, S.H.; Kim, Y.S.; Park, H.G.; Kim, Y.G.; Woo, S.M.; Daniel, D.Y.; Ha, Y.S. Rollover safetyand workable boundary suggestion of an agricultural platform with different attachments. *Agriculture* **2022**, *12*, 1148. [CrossRef]
25. Rondelli, V.; Capacci, E.; Franceschetti, B. Evaluation of the Stability Behavior of an Agricultural Unmanned Ground Vehicle. *Sustainability* **2022**, *14*, 15561. [CrossRef]
26. Majdan, R.; Abrahám, R.; Kollárová, K.; Tkáč, Z.; Matejková, E.; Kubík, Ľ. Alternative Models for Calculation of Static Overturning Angle and Lateral Stability Analysis of Subcompact and Universal Tractors. *Agriculture* **2021**, *11*, 861. [CrossRef]
27. Bietresato, M.; Mazzetto, F. Definition of the Layout for a New Facility to Test the Static and Dynamic Stability of Agricultural Vehicles Operating on Sloping Grounds. *Appl. Sci.* **2019**, *9*, 4135. [CrossRef]

28. Reynolds, S.J.; Groves, W. Effectiveness of roll-over protective structures in reducing farm tractor fatalities. *Am. J. Prev. Med.* **2000**, *18*, 63–69. [CrossRef] [PubMed]
29. Day, L.; Rechnitzer, G.; Lough, J. An Australian experience with tractor rollover protective structure rebate programs: Process, impact and outcome evaluation. *Accid. Anal. Prev.* **2004**, *36*, 861–867. [CrossRef] [PubMed]
30. U.S. Bureau of Labor Statistics. Fatal occupational injuries by industry and event or exposure. In *Injuries, Illnesses, and Fatalities*; U.S. Bureau of Labor Statistics: Washington, DC, USA, 2021.
31. Antunes, S.M.; Cordeiro, C.; Teixeira, H.M. Analysis of fatal accidents with tractors in the Centre of Portugal: Ten years analysis. *Forensic Sci. Int.* **2018**, *287*, 74–80. [CrossRef] [PubMed]
32. Rondelli, V.; Casazza, C.; Martelli, R. Tractor rollover fatalities, analyzing accident scenario. *J. Saf. Res.* **2018**, *67*, 99–106. [CrossRef] [PubMed]
33. Liu, J.; Ayers, P.D. Off-road vehicle rollover and field testing of stability index. *J. Agric. Saf. Health* **1999**, *5*, 59. [CrossRef]
34. Lleras, N.O.; Brennan, S.; Murphy, D.; Klena, M.J.; Garvey, P.M.; Sommer Iii, H.J. Development of an open-source tractor driving simulator for tractor stability tests. *J. Agric. Saf. Health* **2016**, *22*, 227–246.
35. Khoury Junior, J.K.; Souza, C.M.A.D.; Rafull, L.Z.L.; Varella, C.A.A. Simulation of the stability of 2wd agricultural tractors. *Bragantia* **2009**, *68*, 257–267. [CrossRef]
36. Franceschetti, B.; Lenain, R.; Rondelli, V. Comparison between a rollover tractor dynamic model and actual lateral tests. *Biosyst. Eng.* **2014**, *127*, 79–91. [CrossRef]
37. Baek, S.M.; Kim, W.S.; Kim, Y.S.; Baek, S.Y.; Kim, Y.J. Development of a simulation model for HMT of a 50 kW class agricultural tractor. *Appl. Sci.* **2020**, *10*, 4064. [CrossRef]
38. Pawar, N.M.; Velaga, N.R. Modelling the influence of time pressure on reaction time of drivers. *Transp. Res. Part F Traffic Psychol. Behav.* **2020**, *72*, 1–22. [CrossRef]
39. Zheng, E.; Cui, S.; Yang, Y.; Xue, J.; Zhu, Y.; Lin, X. Simulation of the Vibration Characteristics for Agricultural Wheeled Tractor with Implement and Front Axle Hydropneumatic Suspension. *Shock Vib.* **2019**, *2019*, 91345312. [CrossRef]
40. Watanabe, M.; Sakai, K. Identifying tractor overturning scenarios using a driving simulator with a motion system. *Biosyst. Eng.* **2021**, *210*, 261–270. [CrossRef]
41. Gao, J.; Yin, C.; Yuan, G. Warning and active steering rollover prevention control for agricultural wheeled tractor. *PLoS ONE* **2022**, *17*, e028021. [CrossRef] [PubMed]
42. Chowdhury, M.; Ali, M.; Habineza, E.; Reza, M.N.; Kabir, M.S.N.; Lim, S.J.; Choi, I.S.; Chung, S.O. Analysis of Rollover Characteristics of a 12 kW Automatic Onion Transplanter to Reduce Stability Hazards. *Agriculture* **2023**, *13*, 652–669. [CrossRef]
43. Kim, W.S.; Siddique, M.A.A.; Kim, Y.J.; Jung, Y.J.; Baek, S.M.; Baek, S.Y.; Kim, Y.S.; Lim, R.G. Simulation of the Rollover Angle of a Self-Propelled Radish Harvester for Different Load Conditions. *Appl. Sci.* **2022**, *12*, 10733. [CrossRef]
44. Jang, M.K.; Hwang, S.J.; Kim, J.H.; Nam, J.S. Overturning and rollover characteristics of a tractor through dynamic simulations: Effect of slope angle and obstacles on a hard surface. *Biosyst. Eng.* **2022**, *219*, 11–24. [CrossRef]
45. Chowdhury, M.; Islam, M.N.; Iqbal, M.Z.; Islam, S.; Lee, D.H.; Kim, D.G.; Jun, H.J.; Chung, S.O. Analysis of Overturning and Vibration during Field Operation of a Tractor-Mounted 4-Row Radish Collector toward Ensuring User Safety. *Machines* **2020**, *8*, 77. [CrossRef]
46. Kim, Y.; Noh, J.; Shin, S.; Kim, B.; Hong, S. Improved Method for Determining the Height of Center of Gravity of Agricultural Tractors. *J. Biosyst. Eng.* **2016**, *41*, 170–176. [CrossRef]
47. Jung, Y.J.; Lim, R.G.; Choi, C.H.; Kim, Y.J. Analysis of Overturning Angle for Radish Harvester. *Korean Soc. Agric. Mach.* **2019**, *1*, 458–459.
48. Agricultural Machinery Inspection Standards. Available online: https://www.mafra.go.kr/home/5108/subview.do?enc=Zm5jdDF8QEB8JTJGYmJzJTJGaG9tZSUyRjc5MSUyRjU2NTAyNiUyRmFydGNsVmlldy5kbyUzRg== (accessed on 5 January 2023).
49. Song, Y.; Zhang, X.; Wang, W. Rollover dynamics modelling and analysis of self-propelled combine harvester. *Biosyst. Eng.* **2021**, *209*, 271–281. [CrossRef]
50. Larish, C.; Piyabongkarn, D.; Tsourapas, V.; Rajamani, R. A New Predictive Lateral Load Transfer Ratio for Rollover Prevention Systems. *IEEE Trans. Veh. Technol.* **2013**, *62*, 2928–2936. [CrossRef]
51. Fargnoli, M.; Lombardi, M. Safety vision of agricultural tractors: An engineering perspective based on recent studies. *Safety* **2019**, *6*, 1. [CrossRef]
52. Lee, D.G.; Yoo, H.J.; Shin, M.; Oh, J.; Shim, S.B. Analysis of overturning stability of small off-road vehicle. *J. Biosyst. Eng.* **2023**, *48*, 309–318. [CrossRef]
53. *ISO 16231-2:2015*; Self-Propelled Agricultural Machinery—Assessment of Stability—Part 2: Determination of Static Stability and Test Procedures. ISO: Geneva, Switzerland, 2015. Available online: https://www.iso.org/standard/61583.html (accessed on 4 July 2021).